Am J Cancer Res 2026;16(6):2297-2314
www.ajcr.us /ISSN:2156-6976/ajcr0166257

Original Article

METTL14/IGF2BP-mediated m6A methylation of circSLIT2 promotes malignant phenotypes of glioblastoma via the miR-127-5p/SH3GLB1 axis

Lijun Wu[1], Menghao Jin[2], Liangchong Chen[2], Yang Jiang[3], Feng Wang[2]

[1]Clinical Laboratory, Wenzhou Hospital of Integrated Traditional Chinese and Western Medicine, Wenzhou 325000, Zhejiang, China; [2]Department of Neurosurgery, Wenzhou Hospital of Integrated Traditional Chinese and Western Medicine, Wenzhou 325000, Zhejiang, China; [3]Department of Neurosurgery, Shanghai Tenth People's Hospital, Tongji University School of Medicine, Shanghai 200072, China

Received May 22, 2025; Accepted May 11, 2026; Epub June 15, 2026; Published June 30, 2026

Abstract: Glioblastoma is a highly aggressive and lethal brain tumor that typically originates from glial cells, characterized by rapid growth and resistance to treatment, leading to poor patient prognosis. This study investigates the role and mechanism of the newly discovered circular RNA CircSLIT2 in the malignant progression of glioblastoma. We found that circSLIT2 is significantly overexpressed in glioblastoma cell lines and promotes the proliferation, migration, and invasion of glioblastoma cells by regulating miR-127-5p and upregulating SH3GLB1 expression. In vitro experiments demonstrated that the overexpression of circSLIT2 enhanced cell viability, while treatment with miR-127-5p mimics significantly inhibited this effect. Additionally, we confirmed that CircSLIT2 sponges miR-127-5p, reducing its negative regulation of SH3GLB1 and thereby maintaining SH3GLB1's stable expression. We further revealed the critical roles of METTL14 and IGF2BP1 in the m6A methylation and stability of CircSLIT2. Finally, in a nude mouse model, mice with CircSLIT2 overexpression exhibited significantly larger tumor volumes and shorter survival times, providing further evidence of the important role of CircSLIT2 in glioblastoma development and progression. These findings suggest that CircSLIT2 could serve as a potential molecular target, offering new insights for glioblastoma treatment.

Keywords: Glioblastoma, circRNAs, CircSLIT2, miR-127-5p, SH3GLB1, m6A

Introduction

Gliomas are the most common primary malignant brain tumors in the central nervous system, originating from glial cells, including astrocytes, oligodendrocytes, and ependymal cells [1]. Treatment for gliomas is typically individualized based on tumor type, location, and the patient's overall condition, incorporating surgery, radiation therapy, and chemotherapy [2]. However, the prognosis for high-grade gliomas, especially glioblastoma (GBM), remains poor, with high recurrence rates and short survival times [3]. The median survival time is less than 14.6 months. Molecular targeted therapy for GBM is a treatment strategy that targets specific molecular markers in tumor cells, aiming to inhibit tumor growth and dissemination [4]. This therapeutic approach generally works by suppressing key molecules involved in tumor cell survival, proliferation, or angiogenesis [5]. Therefore, identifying key genes associated with the initiation, progression, and malignant phenotypes of GBM and designing targeted therapeutic agents accordingly are crucial directions in molecular targeted therapy research.

Circular RNAs (circRNAs) are a unique class of non-coding RNA molecules that form a closed-loop structure through back-splicing, providing them with high stability and widespread presence in cells [6]. They are involved in regulating gene expression, acting as miRNA sponges, and mediating protein-protein interactions, among other biological processes [7]. In recent years, research has shown that circRNAs exhibit aberrant expression in various diseases, particularly in malignant tumors [8]. For instance,

https://doi.org/10.62347/RNUV4829

circCMTM3 can promote vasculogenic mimicry and malignant progression in glioblastoma [9], while circCOPA can suppress the malignant progression of glioblastoma by encoding novel micropeptides [10]. Given the crucial role of circRNAs in regulating tumor biology, they have become a focal point of cancer research. Further investigation into their functions could help elucidate the molecular mechanisms underlying tumor development and provide novel targets for cancer diagnosis and therapy.

In this study, we identified a novel circular RNA molecule, hsa_circ_0069304, derived from the SLIT2 gene, which we named circSLIT2. CircSLIT2 is significantly overexpressed in glioblastoma and exhibits oncogenic biological effects, promoting malignant phenotypes such as proliferation, invasion, and migration in glioblastoma cells. Mechanistically, circSLIT2 acts as a sponge for miR-127-5p, inhibiting miR-127-5p-mediated degradation of SH3GLB1, leading to the upregulation of SH3GLB1, which subsequently promotes glioma cell malignant progression. Furthermore, our analysis of the aberrant expression of circSLIT2 revealed that METTL14 induces m6A modification of circSLIT2 in glioblastoma cell lines, which is recognized by IGF2BP1, thereby stabilizing circSLIT2 in glioblastoma cells. Therefore, circSLIT2 is a newly discovered oncogenic circRNA in glioblastoma and holds promise as a potential molecular target for glioblastoma therapy.

Materials and methods

Patient samples and ethic

We collected samples from 35 patients with gliomas who were treated at the Neurosurgery Department of Shanghai Tenth People's Hospital from October 2020 to December 2023. This cohort included 11 patients with WHO Grade II gliomas, 12 with Grade III, and 12 with Grade IV. Additionally, we collected 10 adjacent normal brain tissue samples. All fresh surgical specimens were immediately frozen in liquid nitrogen, and diagnoses were confirmed by at least two neuropathologists according to the World Health Organization (WHO) classification criteria. This study was approved by the ethical review committee of Wenzhou Hospital of Integrated Traditional Chinese and Western Medicine (Approval No. 2024-2051).

Cell culture and reagents

The glioblastoma cell line U87 was purchased from the Cell Bank of the Chinese Academy of Sciences (Shanghai, China), and LN229 was obtained from the American Type Culture Collection (ATCC, Manassas, VA, USA). The authenticity of the cell lines was confirmed through short tandem repeat (STR) analysis. The cell lines were cultured in Dulbecco's Modified Eagle Medium (DMEM, HyClone, Logan, UT, USA) supplemented with 10% fetal bovine serum (FBS, Gibco, Carlsbad, CA, USA) and 1% streptomycin/penicillin (Gibco), at 37°C in a 5% CO_2 environment.

Quantitative real-time polymerase chain reaction (qPCR)

According to the manufacturer's instructions, total RNA was extracted using TRIzol reagent (Invitrogen, Carlsbad, CA, USA). Subsequently, complementary DNA (cDNA) was synthesized using the PrimeScript™ RT Reagent Kit with gDNA Eraser (TaKaRa Biotech, Kyoto City, Japan). Real-time PCR was then conducted using TB Green Premix Ex Taq™ II (Tli RNaseH Plus) (Takara) or TaqMan MicroRNA Assays (Thermo Fisher Scientific, Inc.). β-actin was employed as a normalization control, and the results were expressed as 2^(-ΔΔCt). The qPCR reaction conditions were set as follows: initial denaturation at 94°C for 30 s, followed by 40 cycles of denaturation at 94°C for 5 s, annealing at 60°C for 15 s, and extension at 72°C for 10 s. The primer pairs used for qPCR analysis are listed in Supplementary Table 1.

Fluorescence in situ hybridization (FISH)

FISH analysis was carried out following the manufacturer's instructions with the FISH Tag Color Kit (Invitrogen). Oligonucleotide probes designed to target the circSLIT2 junction sequence were synthesized by Gene-Chem (Shanghai, China). U87 and T98G cells were seeded onto glass coverslips that had been treated with poly-D-lysine (Sigma-Aldrich). Images were captured using a precision imaging system that included an ECLIPSE Ts2 fluorescence microscope, a Digital Sight 10 camera, and NIS-Elements software (Nikon, Japan).

RNase R assay

Total RNA was extracted from U87 and T98G cells and subsequently treated with RNase R

enzyme (Geneseed, Guangzhou, China) at a concentration of 20 U/μL. The mixture was then incubated at 37°C for 30 minutes. After this treatment, the total RNA was evaluated using qPCR.

Transfection

The circSLIT2, METTL14, and IGF2BP1 overexpression plasmids were generated using a pLVX vector from GenePharma Co. Ltd. (Shanghai, China). RNA interference (RNAi) was employed to knockdown circSLIT2, SH3GLB1, METTL14, and IGF2BP1, along with their respective negative controls, all designed by Gene-Chem (Shanghai, China). The sequences for all siRNAs can be found in Supplementary Table 2. The mimic, inhibitor, and negative control for miR-127-5p were sourced from Thermo Fisher Scientific (Assay ID: MC20025 and AM20025; Thermo Fisher Scientific, Waltham, MA, USA). U87 and T98G cells that were transfected underwent treatment with puromycin (Sigma, Santa Clara, CA, USA) at a concentration of 10 μg/ml for 15 days, with transfection efficiency confirmed via qPCR.

Cell proliferation assay

Cell proliferation was evaluated using the MTS assay. U87 and T98G cells were seeded in 96-well plates at a density of 10^3 cells per well. At 24, 48, 72, 96, and 120 hours, 20 μl of MTS (Promega, Madison, WI, USA) was added to each well. After a 3-hour incubation period, the absorbance was measured at 495 nm with a UV spectrophotometer (Thermo Fisher Scientific).

5-Ethynyl-2'-deoxyuridine (Edu) proliferation assay

U87 and T98G cells in the exponential growth phase were seeded in 24-well plates at a density of 1×10^5 cells per well and incubated for 24 hours. Following this, the cells were treated with EdU reagent (Beyotime Biotechnology) at 37°C for 2 hours. After treatment, the cells were fixed using paraformaldehyde, and their nuclei were stained with DAPI (Sigma). EdU-positive cells were then visualized using a laser scanning confocal microscope (Olympus, Tokyo, Japan).

Transwell assay and migration assay

In the transwell assay, the upper chamber (8 μm) of the transwell system was coated with 100 μl of Matrigel (BD Biosciences, CA, USA) and incubated at 37°C for 30 minutes. Next, U87 and T98G cells in the exponential growth phase were added to the upper chamber and treated with DMEM containing 0.2% FBS, while the lower chamber was filled with DMEM supplemented with 20% FBS. After a 20-hour incubation, cells in the lower chamber were fixed with 4% paraformaldehyde and stained with hematoxylin and eosin (H&E). The number of invasive U87 and T98G cells was then counted using an inverted microscope (Olympus). For the migration assay, U87 and T98G cells were directly seeded into the upper chamber without Matrigel coating, and the remaining steps adhered to the transwell assay protocol.

Western blotting

The total protein from U87 and T98G cells was obtained using a protein lysis buffer (Beyotime Biotechnology, Beijing, China), and equal amounts of the protein samples (μg) were loaded onto a 10% dodecyl sulfate-polyacrylamide gel for electrophoresis. After electrophoresis, the gels were transferred to a nitrocellulose membrane, which was subsequently blocked with 2% bovine serum albumin (Beyotime Biotechnology). Membranes were incubated overnight at 4°C with primary antibodies against SH3GLB1 (ab180135, 1:1000, Abcam) or β-actin (ab8227, 1:1000, Abcam), followed by incubation with goat anti-rabbit IgG secondary antibody (ab97051, 1:2000, Abcam) on the next day. Finally, the protein bands were detected using an enhanced chemiluminescence (ECL) detection kit (Beyotime Biotechnology), and the band intensities were quantified using Image J software (National Institutes of Health, Bethesda, MD, USA).

Luciferase activity analysis

Predictions for the binding sites between circSLIT2 and miR-127-5p were obtained from the circInterome database (https://circinteractome.nia.nih.gov), while those for the interaction between miR-127-5p and SH3GLB1 were sourced from the miRPathDB database (https://mpd.bioinf.uni-sb.de). Wild-type and mutant

constructs of circSLIT2 and SH3GLB1 were designed and cloned into empty pGL3 vectors. U87 and T98G cells were then plated in 24-well plates and co-transfected with pRL TK (a Renilla luciferase reporter vector, Promega). After 48 hours, the activities of both firefly and Renilla luciferases were measured using a dual-luciferase reporter assay kit (Promega), in accordance with the manufacturer's guidelines.

RNA immunoprecipitation (RIP) assay

The interaction between circSLIT2 and miR-127-5p was assessed using the Magna RIP RNA Binding Protein Immunoprecipitation Kit (Millipore, Darmstadt, Germany) as per the manufacturer's protocol. U87 and T98G cells were lysed with RIP lysis buffer, and the lysates were subjected to treatment with magnetic beads attached to antibodies against Ago2, while IgG was used as a negative control. Following this, the RNAs associated with Ago2 were immunoprecipitated, treated with proteinase K, and analyzed via qPCR to evaluate the enrichment of circSLIT2 and miR-127-5p.

Xenograft experiments

U87 glioma cells overexpressing circSLIT2 or carrying an empty vector were orthotopically injected into the brains of 6-week-old female BALB/c nude mice (Shanghai SLAC Laboratory Animal Co., Ltd., Shanghai, China) at a density of 1 × 10^4 cells per mouse during their exponential growth phase. The mice were observed daily for any neurological symptoms or mortality, and tumor volume was calculated using the formula $V = (D \times d^2)/2$, where D denotes the longest diameter and d denotes the shortest diameter of the tumor. Survival rates across different groups were analyzed using the Log-rank test and Kaplan-Meier analysis. Mice presenting with severe neurological symptoms were euthanized via cervical dislocation. All animal experiments were conducted in accordance with the guidelines provided by the Animal Care Committee of Shanghai Tenth People's Hospital (SHDSYY-2025-6963).

Immunohistochemistry (IHC)

The xenograft tumor samples from the mice were embedded in paraffin and sliced into 4 μm sections. These paraffin-embedded sections were dewaxed, rehydrated, and underwent antigen retrieval, with endogenous peroxidases blocked using an immunohistochemistry method (Beyotime Biotechnology). Primary antibodies targeting Ki-67 or SH3GLB1 (1:100, Abcam) were applied, followed by staining with the DAB Substrate Kit (Abcam). The stained sections were examined under a light microscope (Olympus), and the immunohistochemical results were evaluated according to the German immunohistochemical scoring system [11].

Bioinformatic analyses

The identification of candidate miRNAs for circSLIT2 was carried out using the circIntercome database (https://circinteractome.nia.nih.gov) and the Cancer-Specific CircRNA Database (CSCD, http://geneyun.net/CSCD2/#). For predicting candidate mRNAs associated with miR-127-5p, multiple databases were utilized, including TargetScan (http://www.targetscan.org/vert_71/), MiRDB (http://mirdb.org), miRPathDb 2.0 (https://mpd.bioinf.uni-sb.de/overview.html) and miRWalk (http://mirwalk.umm.uni-heidelberg.de).

Statistical analysis

Statistical analysis and graphical representations were conducted using GraphPad Prism 10.0 (GraphPad Software Inc., San Diego, CA, USA). All experiments were performed in triplicate or more, with results expressed as mean ± standard error. The two-tailed Student's t-test was applied to compare two independent groups. The paired t-test was utilized for matched samples of cancer tissues and paired adjacent non-cancerous tissues from the same patient. Comparisons among multiple groups with a time variable require the use of repeated measures ANOVA. Kaplan-Meier survival curves were plotted to visualize survival outcomes across groups, and the log-rank test was used to determine statistical significance. A *P* value of less than 0.05 was considered statistically significant.

Results

CircSLIT2 is highly expressed in glioblastoma

To analyze the expression and potential mechanism of circRNAs in glioblastoma, we performed circRNA sequencing on three glioblastoma tis-

sues and three normal brain tissues (NBTs). Differential expression analysis was conducted using the limma package, revealing eight upregulated circRNAs (log FC ≥ 2, P < 0.05) and 22 downregulated circRNAs (log FC ≤ -2, P < 0.05) (**Figure 1A-C**; Supplementary Table 3). Among the eight significantly upregulated circRNAs, we focused on hsa_circ_0069304, which exhibited abnormally high expression in glioblastoma, with no prior reports in the literature. Hsa_circ_0069304 is located at chr4:20493383-20600018 in the genome and is formed by back-splicing of exons 24 to 39 of the SLIT2 gene, with a total length of 2917 bp. Therefore, we defined it as circSLIT2 (**Figure 1D**, **1E**). To confirm the back-splicing junction of circSLIT2, Sanger sequencing was performed, which validated its circular structure (**Figure 1F**). We further employed fluorescence in situ hybridization (FISH) to detect the subcellular localization of circSLIT2 in glioblastoma cells, revealing that circSLIT2 was predominantly localized in the cytoplasm (**Figure 1G**). Tissue FISH further demonstrated that circSLIT2 was highly expressed in glioma tissues, while barely detectable in normal brain tissues (**Figure 1H**). Additionally, we conducted RNase R digestion experiments to assess the stability of circSLIT2. The results showed that circSLIT2 levels remained unchanged after RNase R treatment, whereas SLIT2 expression was significantly reduced (**Figure 1I**, **1J**). Furthermore, we collected 15 glioma samples and 15 adjacent normal brain tissues for circSLIT2 expression analysis, finding that circSLIT2 levels were significantly higher in glioma tissues compared to adjacent normal brain tissues (**Figure 1K**). Moreover, in the 35 glioma samples, circSLIT2 expression was positively correlated with WHO grade, with the highest expression observed in WHO grade IV tumors (**Figure 1L**). In summary, circSLIT2 is a novel circRNA that is significantly overexpressed in glioma.

CircSLIT2 promotes malignant progression of glioblastoma cells

To further investigate and confirm the role of circSLIT2 in glioblastoma, we selected two glioblastoma cell lines, U87 and T98G, and performed circSLIT2 overexpression. qPCR was used to confirm the stable and reliable expression levels of circSLIT2 overexpression (**Figure 2A**). We additionally examined the expression level of SLIT2 and observed that circSLIT2 overexpression had no impact on the expression level of SLIT2 (**Figure 2B**). Cell viability assays using MTS revealed that circSLIT2 overexpression significantly enhanced the viability of glioblastoma cells (**Figure 2C**, **2D**). Additionally, the EDU assay demonstrated that circSLIT2 overexpression led to a significant increase in the EDU-positive rate of glioblastoma cells (**Figure 2E**). The Transwell invasion assay showed that circSLIT2 overexpression significantly increased the number of invading glioma cells (**Figure 2F**). Consistently, migration assay results revealed that circSLIT2 overexpression markedly promoted glioma cell migration (**Figure 2G**).

Subsequently, we further explored the effects of circSLIT2 silencing in glioma cell lines. qPCR confirmed that circSLIT2 knockdown significantly downregulated circSLIT2 expression, whereas it exerted no obvious influence on the expression level of SLIT2 (Supplementary Figure 1A, 1B). MTS and EdU assays verified that circSLIT2 silencing notably reduced the proliferative activity and EdU-positive cell ratio of glioma cells (Supplementary Figure 1C-E). Moreover, Transwell invasion and migration assays demonstrated that the numbers of invasive and migratory glioma cells were distinctly decreased following circSLIT2 silencing (Supplementary Figure 1F, 1G). These results strongly suggest that circSLIT2 plays a key role in promoting glioblastoma cell proliferation, invasion, and migration, contributing to the malignant progression of glioblastoma cells.

CircSLIT2 acts as a miRNA sponge for miR-127-5p

To further explore the mechanism by which circSLIT2 promotes the malignant progression of glioblastoma cells, we examined the well-known competing endogenous RNA (ceRNA) mechanism [12]. CircRNAs are known to harbor multiple miRNA response elements (MREs), allowing them to regulate mRNA levels by competitively binding miRNAs. Using the CircInteractome and CSCD databases, we predicted potential miRNAs that may bind to circSLIT2 and identified only one candidate, miR-127-5p (**Figure 3A**). We then performed qPCR to assess the regulatory relationship between miR-127-5p and circSLIT2. The results showed that inhibition of miR-127-5p led to a significant upregu-

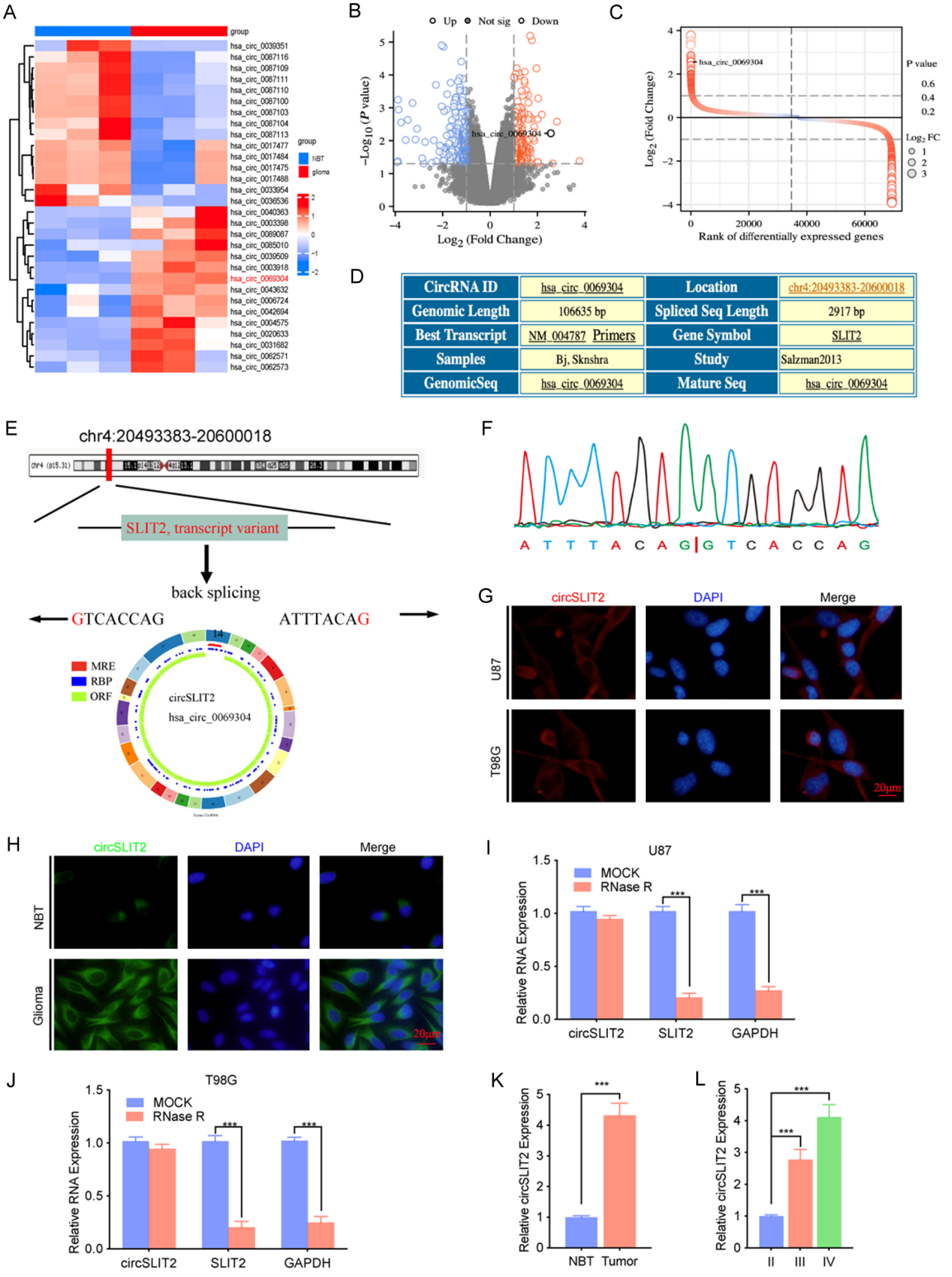

Figure 1. CircSLIT2 is highly expressed in glioblastoma. (A-C) Heatmap (A), volcano plot (B), and differential gene ranking plot (C) displaying circRNA sequencing results in glioblastoma. (D) Basic information of circSLIT2 retrieved from the CircInteractome database. (E) Schematic diagram illustrating the basic structural composition of circSLIT2. (F) Sanger sequencing confirming the circular structure of circSLIT2 with head-to-tail junction. (G) Fluorescence in situ hybridization (FISH) showing the distribution of circSLIT2 in glioma cell lines (With magnification of 40×). Scale bar = 20 μm. (H) FISH assay detecting circSLIT2 expression in normal brain tissues (NBT) and glioma tissues (With

magnification of 40×). Scale bar = 20 μm. (I, J) Expression level changes of circSLIT2 and its linear mRNA SLIT2 after RNase R treatment. (K) qPCR analysis showing the differential expression of circSLIT2 between glioma tissues and adjacent normal brain tissues (n = 15, P < 0.0001, paired t-test). (L) qPCR analysis of circSLIT2 expression levels in WHO grade II (n = 11), grade III (n = 12), and grade IV (n = 12) gliomas. All data are shown as the mean ± SD (three independent experiments). *P < 0.05; **P < 0.01; ***P < 0.001.

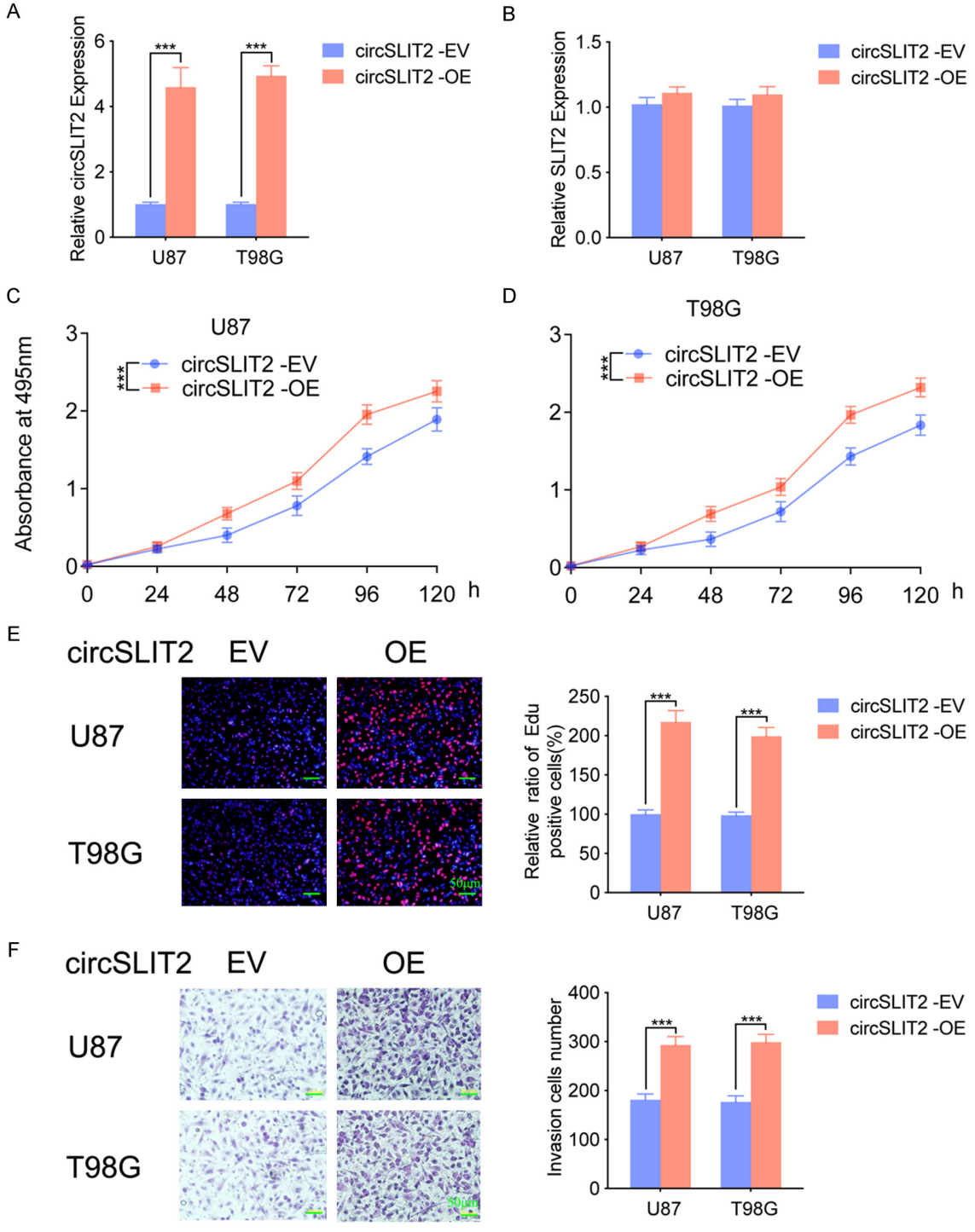

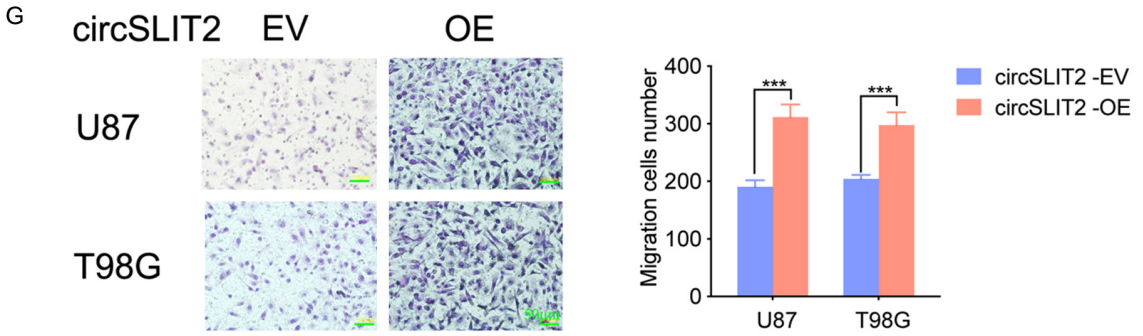

Figure 2. CircSLIT2 promotes malignant progression of glioblastoma cells. (A, B) Validation of circSLIT2 overexpression specificity via qRT-PCR. Compared with empty vector-transfected controls (circSLIT2-EV), U87 and T98G cells transfected with circSLIT2 overexpression vector (circSLIT2-OE) exhibited significantly upregulated expression of circSLIT2 (A), while the level of linear SLIT2 mRNA remained unchanged (B). (C, D) MTS assay measuring absorbance levels after circSLIT2 overexpression in U87 (C) and T98G (D) cells. (E) EDU assay detecting changes in the EDU-positive rate after circSLIT2 overexpression in U87 and T98G cells (With magnification of 20×). Scale bar = 50 μm. (F, G) Transwell (F) and migration (G) assays measuring the number of invasive and migrating cells after circSLIT2 overexpression in U87 and T98G cells (With magnification of 20×). Scale bar = 50 μm. All data are shown as the mean ± SD (three independent experiments). *P < 0.05; **P < 0.01; ***P < 0.001.

lation of circSLIT2 expression in glioblastoma cells, while miR-127-5p mimic treatment significantly downregulated circSLIT2 expression (**Figure 3B**, **3C**). Furthermore, we examined the impact of circSLIT2 on miR-127-5p expression and found that overexpression of circSLIT2 markedly decreased miR-127-5p levels (**Figure 3D**). Based on the CircInteractome database, we identified putative binding sites between circSLIT2 and miR-127-5p (**Figure 3E**), and designed a luciferase reporter assay accordingly. The results demonstrated that miR-127-5p mimic treatment significantly reduced the luciferase activity of circSLIT2, while miR-127-5p inhibitor treatment increased the luciferase activity (**Figure 3F-I**). Finally, we conducted an AGO-RIP assay to determine whether circSLIT2 directly binds to miR-127-5p. The results showed that after miR-127-5p mimic treatment, the enrichment of circSLIT2 and miR-127-5p in the AGO immunoprecipitation group was significantly higher than that in the IgG control group (**Figure 3J-M**). These findings provide strong evidence that circSLIT2 directly binds to and sponges miR-127-5p.

CircSLIT2 promotes the malignant phenotype of glioblastoma cells via miR-127-5p

To confirm whether circSLIT2 promotes the malignant progression of glioblastoma through the regulation of miR-127-5p, we treated glioblastoma cell lines overexpressing circSLIT2 with miR-127-5p mimic. The MTS assay revealed that the increased cell viability induced by circSLIT2 overexpression was suppressed following miR-127-5p mimic treatment (Supplementary Figure 2A, 2B). The EDU assay showed that circSLIT2 overexpression significantly elevated the percentage of EDU-positive cells, indicating enhanced proliferation in glioblastoma cells, whereas miR-127-5p mimic treatment significantly reduced this effect (Supplementary Figure 2C). In both Transwell and migration assays, circSLIT2 overexpression promoted the invasion and migration abilities of glioblastoma cells, while these effects were markedly inhibited following miR-127-5p mimic treatment (Supplementary Figure 2D, 2E).

MiR-127-5p-3p binds to the 3'-UTR of SH3GLB1 mRNA and down-regulates its expression

It is well-known that circRNAs act as molecular sponges for miRNAs, inhibiting miRNA-mediated degradation of downstream target genes to exert their biological effects [13]. To further investigate the mRNAs potentially regulated by miR-127-5p, we used four databases: miRPathDB, miRWalk, miRDB, and TargetScan to predict the targets, identifying nine common mRNAs (**Figure 4A**). We then treated glioblastoma cell lines with miR-127-5p mimic or inhibitor and assessed the expression levels of these

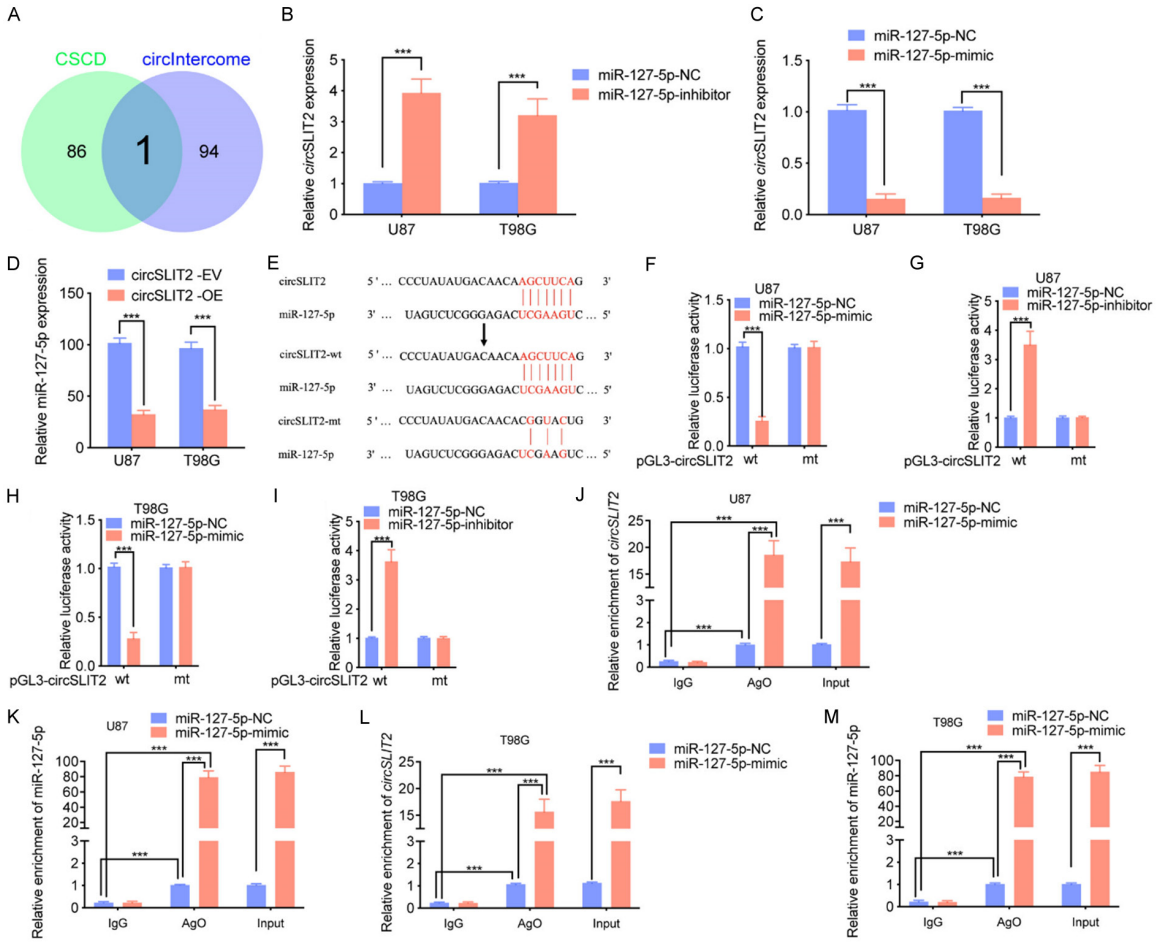

Figure 3. CircSLIT2 acts as a miRNA sponge for miR-127-5p. (A) CSCD and CircInteractome databases predict that circSLIT2 potentially binds to only one miRNA, miR-127-5p. (B, C) qPCR analysis of circSLIT2 expression levels in U87 and T98G cells after treatment with miR-127-5p inhibitor (B) or miR-127-5p mimic (C). (D) qPCR analysis of miR-127-5p expression levels in U87 and T98G cells after circSLIT2 overexpression. (E) Predicted binding site between circSLIT2 and miR-127-5p from the CircInteractome database, with a schematic showing designed mutation sites. (F-I) Luciferase reporter assay measuring circSLIT2 luciferase activity after treatment with miR-127-5p mimic (F, H) or miR-127-5p inhibitor (G, I). (J-M) AGO-RIP assay showing the enrichment levels of circSLIT2 (J, L) and miR-127-5p (K, M) after treatment with miR-127-5p mimic. All data are shown as the mean ± SD (three independent experiments). *P < 0.05; **P < 0.01; ***P < 0.001.

nine mRNAs. Among them, only SH3GLB1 was found to be significantly regulated by miR-127-5p (**Figure 4B-E**). Using western blotting, we further confirmed that SH3GLB1 protein expression was markedly downregulated following miR-127-5p mimic treatment, while it was significantly upregulated after miR-127-5p inhibitor treatment (**Figure 4F**, **4G**). miRPathDB revealed the binding site between miR-127-5p and SH3GLB1 (**Figure 4H**), which was validated using a luciferase reporter assay. The results showed that miR-127-5p mimic treatment significantly reduced the luciferase activity of SH3GLB1, while miR-127-5p inhibitor treatment significantly increased its activity (**Figure 4I-L**). Finally, we examined whether circSLIT2 could regulate SH3GLB1 expression by sponging miR-127-5p. Both qPCR and western blot analyses demonstrated that SH3GLB1 expression was significantly upregulated in circSLIT2-overexpressing cells, but this upregulation was reversed following miR-127-5p mimic treatment (**Figure 4M-P**). These findings confirmed that circSLIT2 stabilizes SH3GLB1 expression by sponging miR-127-5p.

SH3GLB1 promotes the malignant phenotype of glioblastoma cells

Currently, several studies have reported the role of SH3GLB1 in gliomas. For example, SH3GLB1-related autophagy mediates mito-

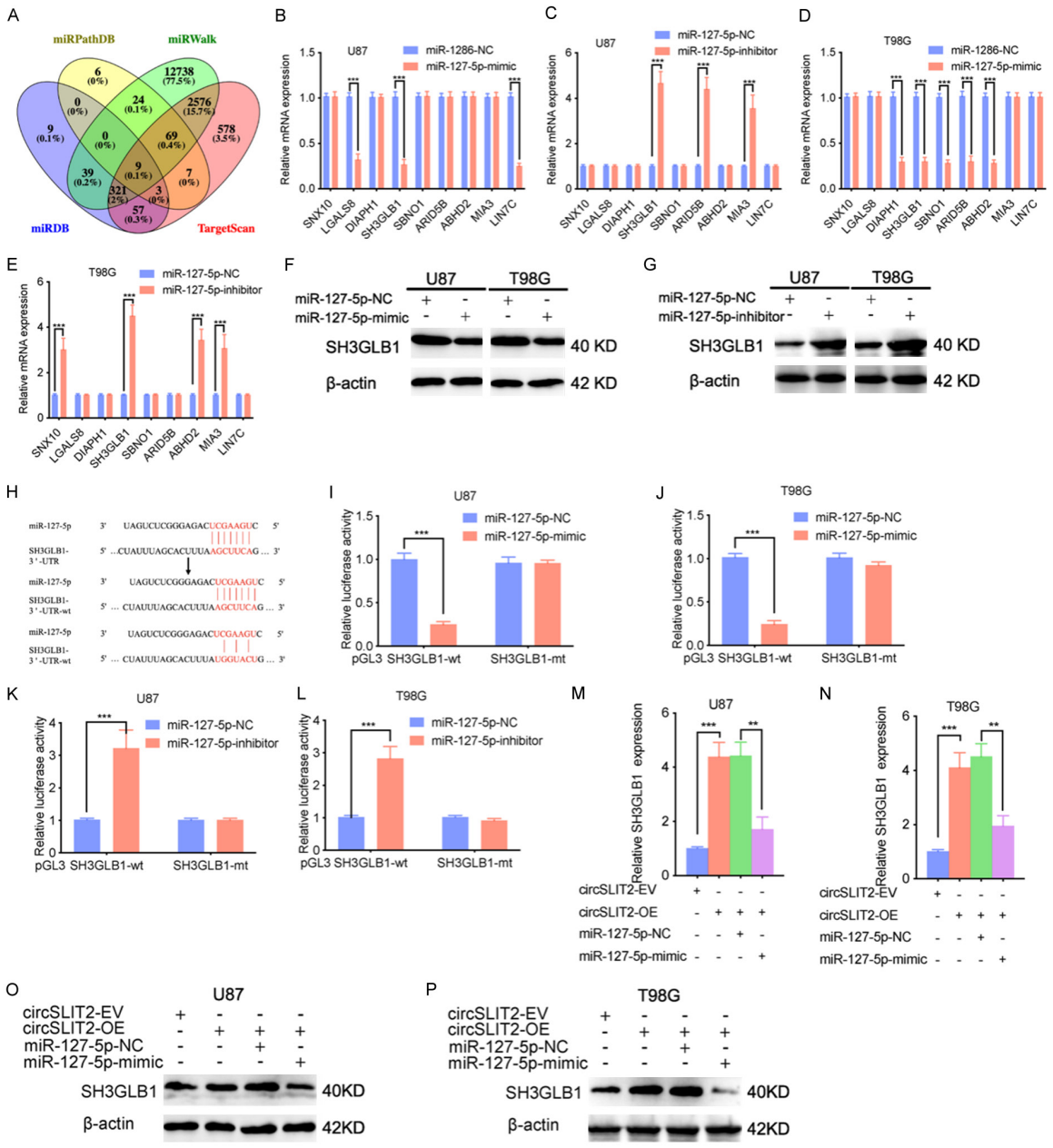

Figure 4. MiR-127-5p-3p binds to the 3'-UTR of SH3GLB1 mRNA and down-regulates its expression. (A) Venn diagram showing nine intersecting mRNA targets (SNX10, LGALS8, DIAPH1, SH3GLB1, SBNO1, ARID5B, ABHD2, MIA3, and LIN7C) predicted by four databases (miRPathDB, miRWalk, miRDB, and TargetScan) to be potential miR-127-5p binding targets. (B-E) qPCR analysis of mRNA levels of the nine candidate target genes in U87 and T98G cells after miR-127-5p mimic (B, D) or miR-127-5p inhibitor (C, E) treatment. (F, G) Western blotting analysis of SH3GLB1 protein levels in U87 and T98G cells after miR-127-5p mimic (F) or miR-127-5p inhibitor (G) treatment. (H) Schematic of the miR-127-5p binding site on SH3GLB1 predicted by the miRPathDB database and the corresponding mutated binding site design. (I-L) Luciferase reporter assay measuring SH3GLB1 luciferase activity in U87 and T98G cells after miR-127-5p mimic (I, J) or miR-127-5p inhibitor (K, L) treatment. (M, N) qPCR analysis of SH3GLB1 mRNA expression in U87 (M) and T98G (N) cells overexpressing circSLIT2 and treated with miR-127-5p mimic. (O, P) Western blotting analysis of SH3GLB1 protein expression in U87 (O) and T98G (P) cells overexpressing circSLIT2 and treated with miR-127-5p mimic. All data are shown as the mean ± SD (three independent experiments). *P < 0.05; **P < 0.01; ***P < 0.001.

chondrial metabolism to confer resistance to temozolomide in glioblastoma [14]. SH3GLB1 can regulate CD133 expression and play a critical role in tumor-initiating cells [15]. However,

direct evidence regarding the biological effects of SH3GLB1 on malignant phenotypes of glioma cells, such as proliferation and invasion, remains lacking. Therefore, we overexpressed SH3GLB1 in glioma cells, and confirmed the successful overexpression by qPCR and western blotting (Supplementary Figure 3A, 3B). MTS and EDU assays showed that SH3GLB1 overexpression significantly enhanced cell proliferative activity (Supplementary Figure 3C-E). Transwell and migration assays demonstrated that the numbers of invasive and migrated cells were markedly increased after SH3GLB1 overexpression (Supplementary Figure 3F, 3G). These findings confirm that SH3GLB1 promotes the malignant progression of glioblastoma cells.

CircSLIT2 promotes the malignant phenotype of glioblastoma cells via SH3GLB1

We further investigated whether circSLIT2 promotes glioblastoma malignancy by sustaining SH3GLB1 expression. Glioblastoma cell lines overexpressing circSLIT2 were treated with SH3GLB1 silencing. MTS assays revealed that the enhanced cell viability induced by circSLIT2 overexpression was significantly inhibited after SH3GLB1 silencing (**Figure 5A**, **5B**). EDU assays showed that circSLIT2 overexpression significantly increased the EDU-positive rate, promoting glioblastoma cell proliferation, while SH3GLB1 silencing led to a significant reduction in the EDU-positive rate (**Figure 5C**). Transwell and migration assays demonstrated that circSLIT2 overexpression enhanced the invasive and migratory abilities of glioblastoma cells, but these effects were markedly suppressed following SH3GLB1 silencing (**Figure 5D**, **5E**).

METTL14 mediates the m6A methylation of circSLIT2 in glioblastoma

We further analyzed and explored the potential mechanisms leading to the high expression of circSLIT2 in glioblastoma. m6A methylation, a common RNA modification, is widely involved in regulating gene expression at multiple levels, including mRNA splicing, stability, transport, and translation [16]. We first conducted MeRIP-qPCR experiments to analyze the m6A modification level of circSLIT2 in glioblastoma cell lines. We found significant enrichment of circSLIT2 after anti-m6A treatment, confirming the presence of notable m6A modification in glioblastoma cell lines (**Figure 6A**). We further performed RIP experiments to analyze potential writers and erasers that may bind to and regulate the m6A modification level of circSLIT2, discovering that only METTL14 could directly bind to circSLIT2 (**Figure 6B**, **6C**). Subsequently, we manipulated METTL14 levels in glioblastoma cell lines. MeRIP-qPCR experiments revealed that silencing METTL14 led to a significant decrease in circSLIT2 enrichment after anti-m6A treatment, while overexpression of METTL14 resulted in a marked increase in circSLIT2 enrichment (**Figure 6D-G**). We further performed qPCR and found that silencing METTL14 significantly decreased the expression level of circSLIT2, while overexpression of METTL14 significantly increased circSLIT2 expression (**Figure 6H**, **6I**). Nuclear run-on assays revealed no significant alterations in circSLIT2 transcription rates in glioma cells with METTL14 overexpression or knockdown, demonstrating that METTL14-mediated circSLIT2 upregulation occurs independently of transcriptional regulation (**Figure 6J**, **6K**). We used SRAMP (sequence-based RNA adenosine methylation site predictor) to predict the specific m6A modification sites on circSLIT2 and identified four potential m6A modification sites (**Figure 6L**, **6M**). Based on these results, we designed circSLIT2 constructs with different mutation sites and conducted MeRIP-qPCR. We found that only mutations at sites 3 and 4 significantly downregulated the m6A levels of circSLIT2, indicating that m6A modification occurs at the adenine residues at positions 1351 and 2338 (**Figure 6N**, **6O**).

IGF2BP1 recognizes m6A-modified circSLIT2 and maintains its stability

Although the above studies revealed that METTL14 promotes the m6A modification of circSLIT2 in glioblastoma cell lines, the specific reader genes that maintain its high expression require further investigation. Given that we observed in **Figure 1G** that the expression of circSLIT2 is primarily localized in the cytoplasm, we focused on analyzing reader molecules involved in m6A modification that are predominantly distributed in the cytoplasm and play roles in mRNA processing, transcription, or stability. This analysis included molecules such as YTHDF1, YTHDF3, and IGF2BP1/2/3.

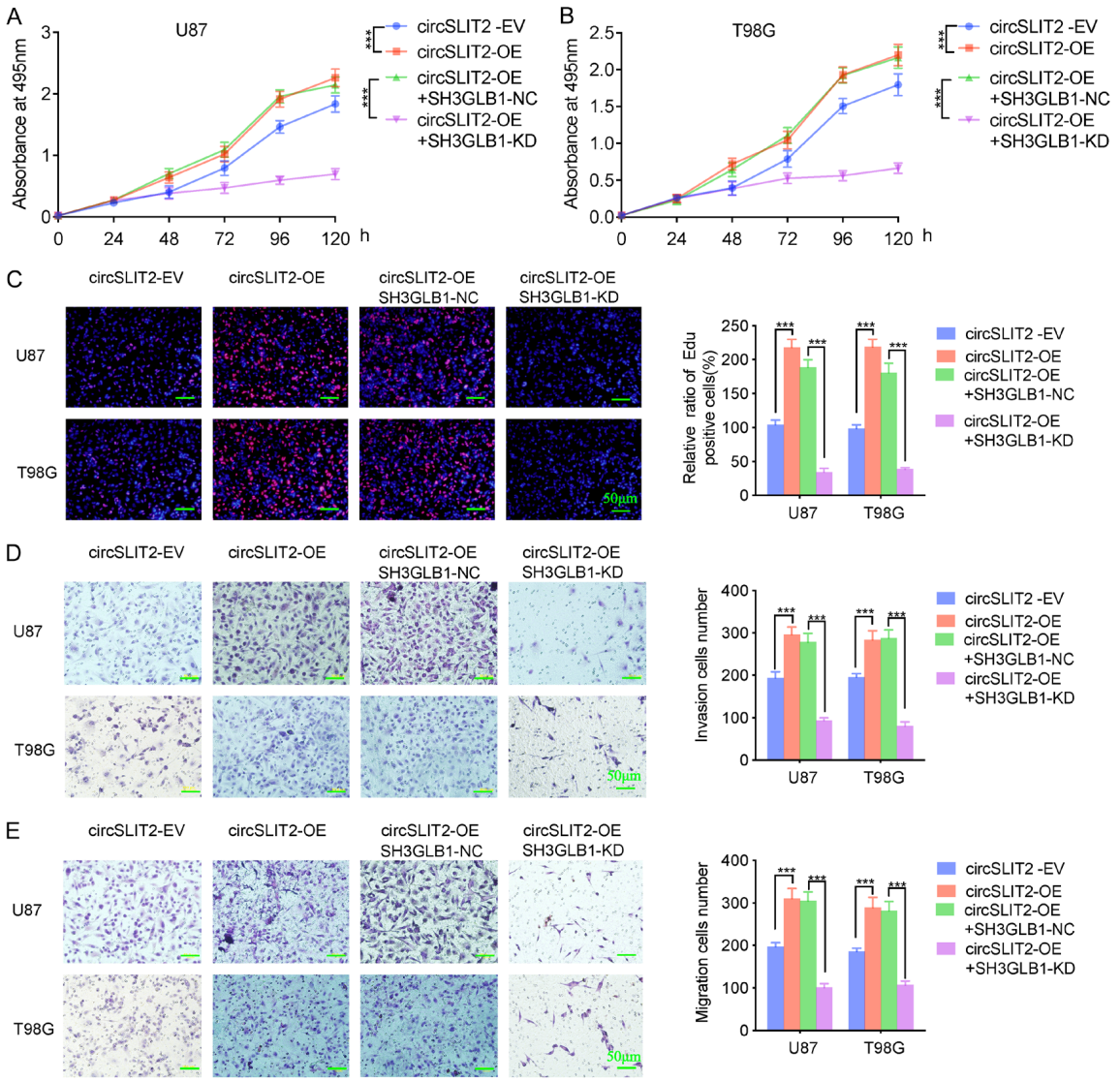

Figure 5. CircSLIT2 promotes the malignant phenotype of glioblastoma cells via SH3GLB1. (A, B) MTS assay measuring changes in absorbance levels in U87 and T98G cells overexpressing circSLIT2 after SH3GLB1 silencing. (C) EDU assay detecting changes in EDU-positive cell rates in U87 and T98G cells overexpressing circSLIT2 after SH3GLB1 silencing (With magnification of 20×). Scale bar = 50 μm. (D, E) Transwell and migration assays showing changes in cell invasion (D) and migration (E) in U87 and T98G cells overexpressing circSLIT2 after SH3GLB1 silencing (With magnification of 20×). Scale bar = 50 μm. All data are shown as the mean ± SD (three independent experiments). *P < 0.05; **P < 0.01; ***P < 0.001.

RIP experiments showed that only after anti-IGF2BP1 treatment could we detect the enrichment of circSLIT2, suggesting that circSLIT2 can bind to the m6A reader IGF2BP1 (**Figure 6P**, **6Q**). qPCR analysis revealed that overexpression of IGF2BP1 significantly upregulated the expression level of circSLIT2, while silencing IGF2BP1 led to a marked downregulation of circSLIT2 (**Figure 6R**, **6S**). Furthermore, we conducted RNA stability assays and found that overexpression of IGF2BP1 significantly prolonged the half-life of circSLIT2, indicating that IGF2BP1 can promote and maintain the stability of circSLIT2 (**Figure 6T**, **6U**). These experimental results provide strong evidence that METTL14 can induce the m6A modification of circSLIT2 in glioblastoma cell lines, which can subsequently be recognized by IGF2BP1, thereby maintaining the stability of circSLIT2 in these cells.

CircSLIT2/miR-127-5p/SH3GLB1 axis regulates glioblastoma tumorigenesis in vivo

Although our previous experiments confirmed that CircSLIT2 promotes the malignant pro-

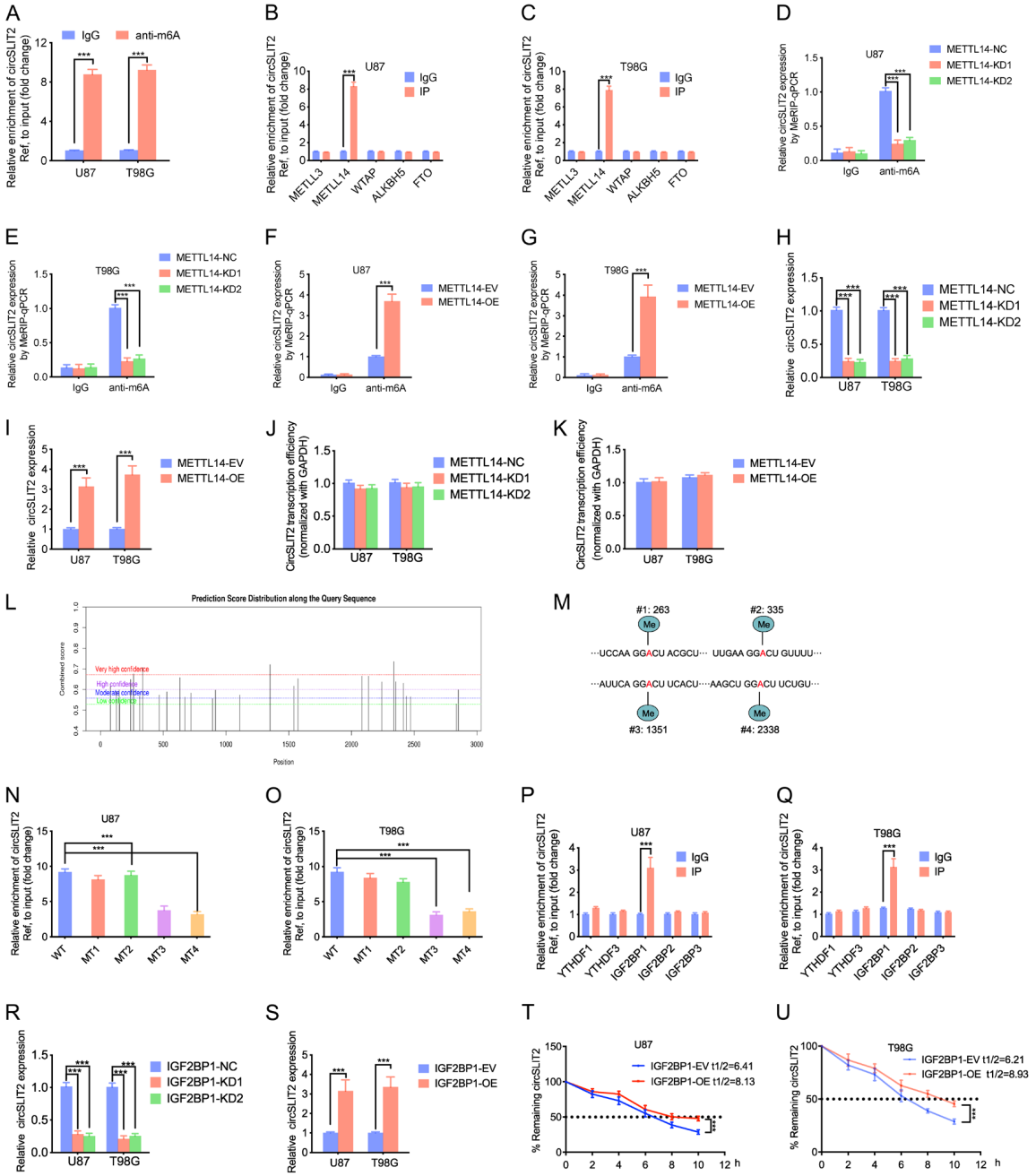

Figure 6. CircSLIT2 is regulated by the METTL14/IGF2BP1-mediated m6A methylation. (A) MeRIP-qPCR analysis showing the level of m6A modification on circSLIT2 in U87 and T98G cells. (B, C) RIP assay detecting potential interactions between circSLIT2 and m6A writers or erasers in U87 and T98G cells. (D-G) MeRIP-qPCR analysis showing the changes in m6A modification levels of circSLIT2 after METTL14 knockdown (D, E) or overexpression (F, G) in U87 and T98G cells. (H, I) qPCR analysis showing the expression levels of circSLIT2 after METTL14 knockdown (H) or overexpression (I) in U87 and T98G cells. (J, K) Transcription efficiency of circSLIT2 in U87 and T98G cells with METTL14 knockdown (J) or overexpression (K), normalized to GAPDH. ns, not significant. (L) SRAMP prediction showing potential m6A methylation sites on the circSLIT2 molecule. (M) Schematic of designed mutations at the four predicted m6A modification sites with the highest likelihood. (N, O) MeRIP-qPCR analysis showing changes in m6A modification levels on circSLIT2 after mutating the different predicted m6A sites. (P, Q) RIP assay detecting potential interactions between circSLIT2 and m6A readers promoting RNA stability or expression in U87 and T98G cells. (R, S) qPCR analysis showing circSLIT2 expression levels after IGF2BP1 knockdown (R) or overexpression (S) in U87 and T98G cells. (T, U) Actinomycin D assay measuring the half-life of circSLIT2 after IGF2BP1 overexpression in U87 (T) and T98G (U) cells. All data are shown as the mean ± SD (three independent experiments). *P < 0.05; **P < 0.01; ***P < 0.001.

gression of glioblastoma cells, including proliferation, invasion, and migration, through the sponge adsorption of miR-127-5p to upregulate SH3GLB1 at the cellular level, there was a lack of validation at the animal model level. We further conducted intracranial tumorigenesis experiments in nude mice. After inoculating the U87 glioblastoma cell line with overexpressed CircSLIT2, we observed that the volume of the tumors formed in the nude mice was significantly larger than that of the control group (**Figure 7A**, **7B**). Kaplan-Meier survival analysis indicated that the survival time of mice inoculated with CircSLIT2-overexpressing U87 cells was markedly shorter than that of the control group (**Figure 7C**). qPCR analysis of the intracranial tumor tissues revealed that the expression levels of CircSLIT2 and SH3GLB1 were significantly elevated in the CircSLIT2 overexpression group (**Figure 7D**, **7E**), while the expression level of miR-127-5p was significantly downregulated (**Figure 7F**). Furthermore, immunohistochemical analysis showed that the staining intensity of the proliferation marker Ki-67 and SH3GLB1 was significantly higher in the CircSLIT2 overexpression group compared to the control group (**Figure 7G**, **7H**). These results from the in vivo experiments in nude mice strongly confirm that CircSLIT2 plays a crucial role in promoting the occurrence and development of glioblastoma (**Figure 7I**).

Discussion

Circular RNAs (circRNAs) are a newly discovered class of non-coding RNAs with a unique closed-loop structure that makes them highly stable and resistant to degradation by exonucleases [17]. In various tumors, circRNAs have been found to play important regulatory roles, particularly in the initiation and progression of malignant gliomas, where their functions are gradually being uncovered [18]. Studies have shown that circRNAs can influence glioma cell behavior by sponging microRNAs, regulating gene expression, and interacting with proteins [19]. Specifically, some circRNAs regulate tumor cell proliferation, migration, and invasion, and are also associated with forms of cell death such as apoptosis and ferroptosis [20]. Furthermore, circRNAs play a critical role in the metabolic reprogramming of gliomas by influencing pathways like iron homeostasis and lipid peroxidation, which modulate the sensitivity of tumor cells to ferroptosis [21]. Due to their stability and diverse functions, circRNAs are considered potential biomarkers and therapeutic targets for tumors. In-depth investigation of the mechanisms of circRNAs in gliomas could provide novel insights into the diagnosis and treatment of this aggressive cancer.

In this study, we identified a novel circular RNA molecule, hsa_circ_0069304, which is significantly overexpressed in glioblastoma. Both in vitro cell experiments and in vivo mouse models demonstrated that its overexpression promotes malignant phenotypes such as proliferation, invasion, and migration in glioblastoma. Currently, there are no reports of hsa_circ_0069304 in any malignancy, but its host gene, SLIT2, has been associated with other circSLIT2 homologs. For instance, circSLIT2 has been reported in gastric cancer, where it is significantly overexpressed and serves as a predictor of poor prognosis in patients, though the specific hsa-circ name was not mentioned in the article, making it unclear which exact circSLIT2 variant was involvedreatic ductal adenocarcinoma [22]. Another circSLIT2 isoform, hsa_circ_0009113, is significantly overexpressed and promotes malignant progression by regulating aerobic glycolysis via the miR-510-5p/c-Myc/LDHA axis [23]. These studies consistently demonstrate high circSLIT2 expression in various malignancies, where it contributes to cancer progression and poor prognosis, which aligns with our findings in glioblastoma.

MiRNAs are an important class of non-coding RNAs that regulate gene expression post-transcriptionally by targeting specific mRNAs, thus influencing glioma development and progression [24]. Studies have shown that miRNAs exhibit abnormal expression in gliomas, potentially playing a role in regulating key processes such as cell proliferation, migration, invasion, and apoptosis [25]. In this study, we used bioinformatics predictions and molecular biology experiments to demonstrate that circSLIT2 acts as a sponge for miR-127-5p, inhibiting miR-127-5p-mediated degradation of SH3GLB1, leading to the upregulation of SH3GLB1 and promoting the malignant progression of glioma cells. Although no studies have yet reported on miR-127-5p in gliomas, it has been implicated in other malignancies. For example, long non-coding RNA AC006329.1 sponges miR-127-5p

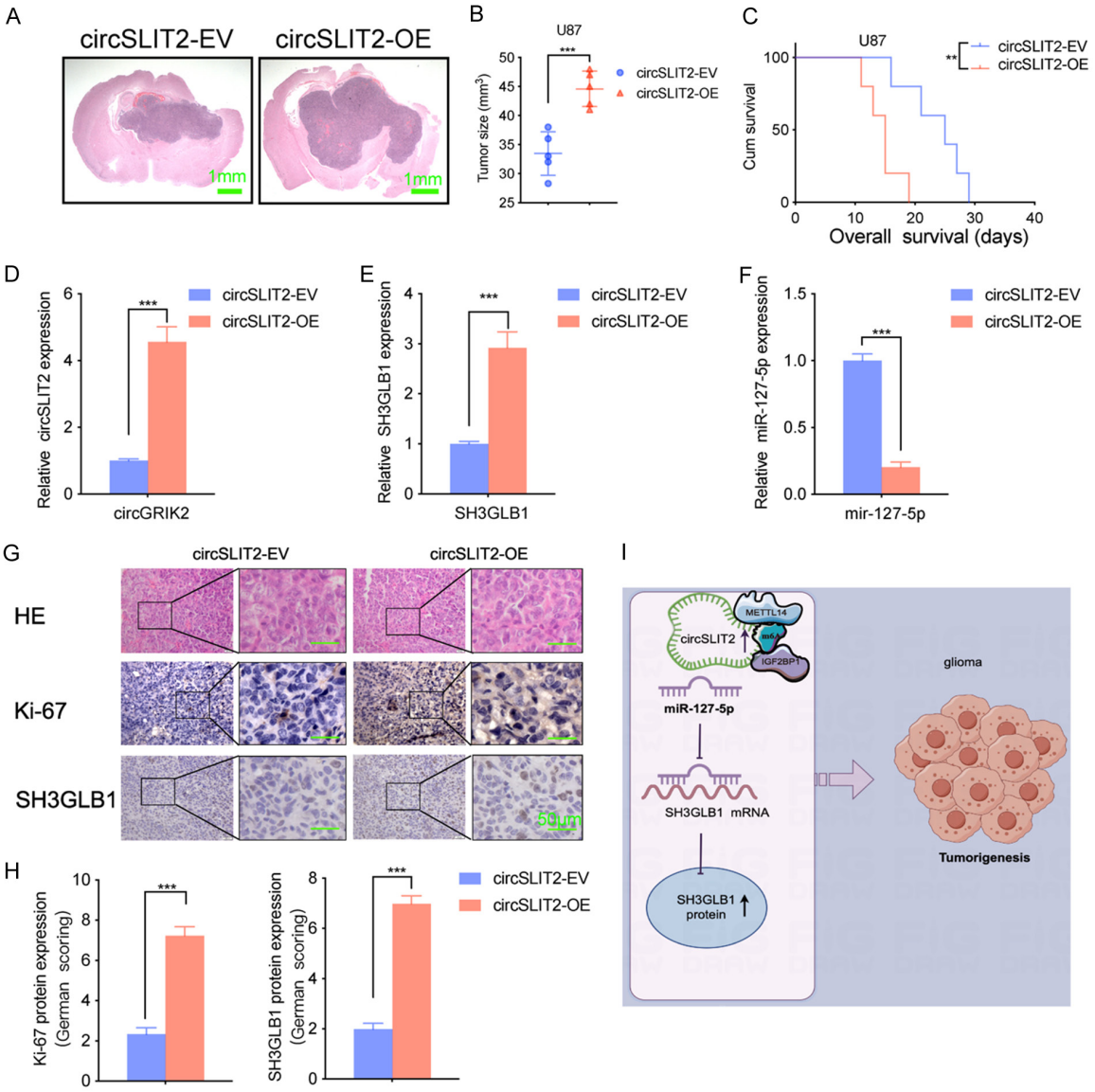

Figure 7. CircSLIT2/miR-127-5p/SH3GLB1 axis regulates glioblastoma tumorigenesis in vivo. (A) Representative coronal HE-stained images showing the intracranial tumor size after circSLIT2 overexpression (With magnification of 5×). Scale bar = 1 mm. (B) Quantification of tumor volume after circSLIT2 overexpression. (C) Kaplan-Meier survival curve showing the effect of circSLIT2 overexpression on mouse survival outcomes. (D-F) qPCR analysis showing the expression levels of circSLIT2 (D), SH3GLB1 (E), and miR-127-5p (F) in intracranial tumor tissues from mice overexpressing circSLIT2. (G) Representative HE staining and immunohistochemistry (IHC) images showing changes in Ki-67 and SH3GLB1 staining intensity in intracranial tumor tissues from mice overexpressing circSLIT2 (With magnification of 10× and 40×). Scale bar = 50 μm. (H) Quantitative analysis of Ki-67 and SH3GLB1 IHC staining using the German immunohistochemical scoring system. (I) Schematic model illustrating that METTL14 promotes m6A modification of circSLIT2, which is recognized and stabilized by IGF2BP1, leading to circSLIT2 overexpression. circSLIT2 acts as a sponge for miR-127-5p, resulting in increased SH3GLB1 expression and promoting glioblastoma progression. All data are shown as the mean ± SD (three independent experiments). *P < 0.05; **P < 0.01; ***P < 0.001.

to promote the malignant progression and metastasis of hepatocellular carcinoma [26]. Additionally, hsa_circ_0006732 regulates RAB3D expression by sponging miR-127-5p, promoting proliferation, invasion, and epithelial-mesenchymal transition (EMT) in colorectal cancer cells [27]. In our study, the malignant phenotypes induced by circSLIT2 overexpres-

sion, such as glioblastoma cell proliferation, invasion, and migration, were effectively blocked by miR-127-5p mimics, suggesting that miR-127-5p plays a tumor-suppressive role in gliomas, consistent with its effects in other cancers.

The SH3GLB1 gene encodes SH3-domain binding protein 1, also known as Bif-1, which plays a crucial role in apoptosis, autophagy, and dynamic remodeling of the cell membrane [28]. SH3GLB1 participates in apoptosis by interacting with BAX and BCL-2 family proteins, promoting mitochondrial membrane permeability changes and inducing cell death [29]. Additionally, it regulates the formation and maturation of autophagosomes, thus contributing to the autophagy process and maintaining intracellular homeostasis. Studies indicate that SH3GLB1 has critical regulatory functions in various cancers, and its abnormal expression is closely associated with tumorigenesis and progression, making it a potential therapeutic target. In glioma stem cells, SH3GLB1 upregulates CD133 expression via histone H4K5 acetylation, facilitating the formation of tumor-initiating cells [15]. Silencing SH3GLB1 inhibits glioma cell proliferation, migration, and invasion, and enhances sensitivity to Temozolomide [30]. The expression of SH3GLB1 increases with glioma grade and is closely linked to poor patient prognosis, contributing to Temozolomide resistance through mitochondrial metabolism [14]. Thus, our study supports that circSLIT2 promotes glioma progression by sponging miR-127-5p, leading to the upregulation of SH3GLB1, with strong logical and experimental evidence.

N6-methyladenosine (m6A) methylation refers to the methylation of the adenosine base at the N6 position in RNA molecules, which is one of the most common RNA modifications [31]. It plays a crucial role in regulating RNA stability, splicing, and translation efficiency. Recent studies have shown that m6A modifications also occur in circRNAs, influencing their biogenesis, transport, and degradation, thereby affecting their function [32]. m6A modifications can alter interactions between circRNAs and binding proteins, thereby regulating cellular behaviors, particularly in tumorigenesis and cancer progression. Investigating the regulatory mechanisms of m6A methylation on circRNAs could help elucidate their roles in cancer, offering new insights for precision medicine [33]. For example, METTL14-dependent m6A methylation was shown to downregulate circUGGT2 expression in gastric cancer, suppressing malignant progression [34]. In lung cancer, METTL3-induced m6A modification of circ_0000620 leads to its high expression, which in turn enhances cisplatin resistance and inhibits apoptosis, contributing to cancer progression [35]. In ischemic brain tissues, the m6A modification level of circOGDH was significantly elevated. IGF2BP1 maintained the high expression of circOGDH in the ischemic penumbra by enhancing its RNA stability, thereby exacerbating the brain tissue injury response [36]. In this study, we discovered that METTL14 facilitates the m6A modification of circSLIT2 in glioblastoma cell lines. The m6A-modified circSLIT2 is recognized by IGF2BP1, which maintains the stability of circSLIT2 in glioblastoma cells. IGF2BP1, an "m6A reader", stabilizes specific mRNAs by recognizing m6A modification sites and enhancing their translation. IGF2BP1 is highly expressed in various cancers and promotes tumor cell proliferation and metastasis. For instance, in glioblastoma, the m6A reader protein IGF2BP1 can bind to circSPECC1, promoting its expression and stability [37]. In gastric cancer, IGF2BP1 regulates T lymphocytes' antitumor immunity by maintaining NRF2 mRNA stability through the METTL5/m6A/NRF2 axis [38].

Conclusion

In this study, we identified a novel circular RNA, circSLIT2, which is significantly overexpressed in glioblastoma and promotes malignant phenotypes such as tumor proliferation, invasion, and migration. Mechanistically, circSLIT2 acts as a sponge for miR-127-5p, inhibiting the degradation of SH3GLB1, thereby driving tumor progression. Additionally, circSLIT2 undergoes m6A modification induced by METTL14, which is recognized by IGF2BP1, ensuring its stability in tumor cells. These findings suggest that circSLIT2 is a key oncogenic factor in glioblastoma and may serve as a potential target for future molecular therapies.

Acknowledgements

This work was supported by the Wenzhou Basic Public Welfare Research Project (grant number 2024Y1074).

Written informed consent was obtained from all enrolled patients

Disclosure of conflict of interest

None.

Abbreviations

GBM, glioblastoma; NBTs, normal brain tissues; circRNA, circular RNA; miRNAs, microRNAs; ceRNAs, competing endogenous RNAs; MRE, miRNA response elements; m6A modification, N6-methyladenosine (m6A); FISH, fluorescence in situ hybridization; H&E stain, hematoxylin and eosin stain; IHC, Immunohistochemistry; qRT-PCR/qPCR, Real-Time Quantitative Reverse Transcription polymerase chain reaction; WHO, World Health Organization; STR, short tandem repeat; DMEM, Dulbecco's Modified Eagle Medium; FBS, fetal bovine serum; cDNA, complementary DNA; RNAi, RNA interference; ECL, enhanced chemiluminescence.

Address correspondence to: Feng Wang, Department of Neurosurgery, Wenzhou Hospital of Integrated Traditional Chinese and Western Medicine, No. 75 Jinxiu Road, Lucheng District, Wenzhou 325000, Zhejiang, China. Tel: +86-0577-8891-0614; E-mail: wangfeng185362@163.com; Yang Jiang, Department of Neurosurgery, Shanghai Tenth People's Hospital, Tongji University School of Medicine, No. 301 Yanchang Road, Jing'an District, Shanghai 200072, China. Tel: +86-021-6630-3232; E-mail: windjy0523@tongji.edu.cn

References

[1] Karimi-Sani I, Molavi Z, Naderi S, Mirmajidi SH, Zare I, Naeimzadeh Y, Mansouri A, Tajbakhsh A, Savardashtaki A and Sahebkar A. Personalized mRNA vaccines in glioblastoma therapy: from rational design to clinical trials. J Nanobiotechnology 2024; 22: 601.

[2] Hotchkiss KM, Karschnia P, Schreck KC, Geurts M, Cloughesy TF, Huse J, Duke ES, Lathia J, Ashley DM, Nduom EK, Long G, Singh K, Chalmers A, Ahluwalia MS, Heimberger A, Bagley S, Todo T, Verhaak R, Kelly PD, Hervey-Jumper S, de Groot J, Patel A, Fecci P, Parney I, Wykes V, Watts C, Burns TC, Sanai N, Preusser M, Tonn JC, Drummond KJ, Platten M, Das S, Tanner K, Vogelbaum MA, Weller M, Whittle JR, Berger MS and Khasraw M. A brave new framework for glioma drug development. Lancet Oncol 2024; 25: e512-e519.

[3] Alnahhas I. Molecular testing in gliomas: what is necessary in routine clinical practice? Curr Oncol Rep 2024; 26: 1277-1282.

[4] Stitzlein LM, Adams JT, Stitzlein EN, Dudley RW and Chandra J. Current and future therapeutic strategies for high-grade gliomas leveraging the interplay between epigenetic regulators and kinase signaling networks. J Exp Clin Cancer Res 2024; 43: 12.

[5] van den Bent MJ, Geurts M, French PJ, Smits M, Capper D, Bromberg JEC and Chang SM. Primary brain tumours in adults. Lancet 2023; 402: 1564-1579.

[6] Yi Q, Feng J, Lan W, Shi H, Sun W and Sun W. CircRNA and lncRNA-encoded peptide in diseases, an update review. Mol Cancer 2024; 23: 214.

[7] Wang Y, Zhang J, Yang Y, Liu Z, Sun S, Li R, Zhu H, Li T, Zheng J, Li J and Ma L. Circular RNAs in human diseases. MedComm (2020) 2024; 5: e699.

[8] Sun Q, Lei X and Yang X. CircRNAs as upstream regulators of miRNA//HMGA2 axis in human cancer. Pharmacol Ther 2024; 263: 108711.

[9] Wang C, Liu Y, Zuo Z, Cui D, Xu Y, Li L and Jiang Y. Dual role of exosomal circCMTM3 derived from GSCs in impeding degradation and promoting phosphorylation of STAT5A to facilitate vasculogenic mimicry formation in glioblastoma. Theranostics 2024; 14: 5698-5724.

[10] Peng D, Wei C, Jing B, Yu R, Zhang Z and Han L. A novel protein encoded by circCOPA inhibits the malignant phenotype of glioblastoma cells and increases their sensitivity to temozolomide by disrupting the NONO-SFPQ complex. Cell Death Dis 2024; 15: 616.

[11] Jiang Y, Zhou J, Hou D, Luo P, Gao H, Ma Y, Chen YS, Li L, Zou D, Zhang H, Zhang Y and Jing Z. Prosaposin is a biomarker of mesenchymal glioblastoma and regulates mesenchymal transition through the TGF-beta1/Smad signaling pathway. J Pathol 2019; 249: 26-38.

[12] Qattan A, Al-Tweigeri T, Suleman K, Alkhayal W and Tulbah A. Advanced insights into competitive endogenous RNAs (ceRNAs) regulated pathogenic mechanisms in metastatic triple-negative breast cancer (mTNBC). Cancers (Basel) 2024; 16: 3057.

[13] Martínez-Espinosa I, Serrato JA and Ortiz-Quintero B. MicroRNAs in lung cancer brain metastasis. Int J Mol Sci 2024; 25: 10325.

[14] Chien CH, Yang WB, Chuang JY, Lee JS, Liao WA, Huang CY, Chen PY, Wu AC, Yang ST, Lai CC, Chi PI, Chu JM, Cheng SM, Liu CC, Hwang DY, Chen SH and Chang KY. SH3GLB1-related autophagy mediates mitochondrial metabolism to acquire resistance against temozolomide in glioblastoma. J Exp Clin Cancer Res 2022; 41: 220.

[15] Chien CH, Lai CC, Chuang JY, Chu JM, Liu CC and Chang KY. Role of SH3GLB1 in the regulation of CD133 expression in GBM cells. BMC Cancer 2023; 23: 713.
[16] Xie GS and Richard HT. m(6)A mRNA modifications in glioblastoma: emerging prognostic biomarkers and therapeutic targets. Cancers (Basel) 2024; 16: 727.
[17] Mafi A, Hedayati N, Kahkesh S, Khoshayand S, Alimohammadi M, Farahani N and Hushmandi K. The landscape of circRNAs in gliomas temozolomide resistance: insights into molecular pathways. Noncoding RNA Res 2024; 9: 1178-1189.
[18] Hsu CY, Faisal A, Jumaa SS, Gilmanova NS, Ubaid M, Athab AH, Mirzaei R and Karampoor S. Exploring the impact of circRNAs on cancer glycolysis: insights into tumor progression and therapeutic strategies. Noncoding RNA Res 2024; 9: 970-994.
[19] Tang C, He X, Jia L and Zhang X. Circular RNAs in glioma: molecular functions and pathological implications. Noncoding RNA Res 2023; 9: 105-115.
[20] Tirpe A, Streianu C, Tirpe SM, Kocijancic A, Pirlog R, Pirlog B, Busuioc C, Pop OL and Berindan-Neagoe I. The Glioblastoma CircularRNAome. Int J Mol Sci 2023; 24: 14545.
[21] Wang X, Wang J, An Z, Yang A, Qiu M and Tan Z. CircXPO1 Promotes Glioblastoma Malignancy by Sponging miR-7-5p. Cells 2023; 12: 831.
[22] Wang L, Xiao S, Zheng Y and Gao Z. CircRNA circSLIT2 is a novel diagnostic and prognostic biomarker for gastric cancer. Wien Klin Wochenschr 2023; 135: 472-477.
[23] Guan H, Luo W, Liu Y and Li M. Novel circular RNA circSLIT2 facilitates the aerobic glycolysis of pancreatic ductal adenocarcinoma via miR-510-5p/c-Myc/LDHA axis. Cell Death Dis 2021; 12: 645.
[24] Yang L, Niu Z, Ma Z, Wu X, Vong CT, Li G and Feng Y. Exploring the clinical implications and applications of exosomal miRNAs in gliomas: a comprehensive study. Cancer Cell Int 2024; 24: 323.
[25] Palizkaran Yazdi M, Barjasteh A and Moghbeli M. MicroRNAs as the pivotal regulators of Temozolomide resistance in glioblastoma. Mol Brain 2024; 17: 42.
[26] Kong XX, Yang X, Jiang WJ, Zhu M and Kong LB. The Long Non-Coding RNA AC006329.1 facilitates hepatocellular carcinoma progression and metastasis by regulating miR-127-5p/SHC3/ERK axis. J Hepatocell Carcinoma 2023; 10: 1085-1103.
[27] Yang T, Sun J, Wang W, Li D, Yang X, Jia A, Ma Y and Fan Z. Hsa_circ_0006732 regulates colorectal cancer cell proliferation, invasion and EMT by miR-127-5p/RAB3D axis. Mol Cell Biochem 2022; 477: 2751-2760.
[28] Takahashi Y, Meyerkord CL and Wang HG. Bif-1/endophilin B1: a candidate for crescent driving force in autophagy. Cell Death Differ 2009; 16: 947-955.
[29] Gao A, Zou J, Mao Z, Zhou H and Zeng G. SUMO2-mediated SUMOylation of SH3GLB1 promotes ionizing radiation-induced hypertrophic cardiomyopathy through mitophagy activation. Eur J Pharmacol 2022; 924: 174980.
[30] Zhang H, Lu X, Wang N, Wang J, Cao Y, Wang T, Zhou X, Jiao Y, Yang L, Wang X, Cong L, Li J, Li J, Ma HP, Pan Y, Ning S and Wang L. Autophagy-related gene expression is an independent prognostic indicator of glioma. Oncotarget 2017; 8: 60987-61000.
[31] Pan T, Wu F, Li L, Wu S, Zhou F, Zhang P, Sun C and Xia L. The role m(6)A RNA methylation is CNS development and glioma pathogenesis. Mol Brain 2021; 14: 119.
[32] Wang J, Sha Y and Sun T. m(6)A modifications play crucial roles in glial cell development and brain tumorigenesis. Front Oncol 2021; 11: 611660.
[33] Galardi S, Michienzi A and Ciafrè SA. Insights into the regulatory role of m(6)A epitranscriptome in glioblastoma. Int J Mol Sci 2020; 21: 2816.
[34] Chen XY, Yang YL, Yu Y, Chen ZY, Fan HN, Zhang J and Zhu JS. CircUGGT2 downregulation by METTL14-dependent m(6)A modification suppresses gastric cancer progression and cisplatin resistance through interaction with miR-186-3p/MAP3K9 axis. Pharmacol Res 2024; 204: 107206.
[35] Li X, Wang Y, Cheng J, Qiu L, Wang R, Zhang Y and Wang H. METTL3 -mediated m6A modification of circ_0000620 regulates cisplatin sensitivity and apoptosis in lung adenocarcinoma via the MiR-216b-5p/KRAS axis. Cell Signal 2024; 123: 111349.
[36] Su X, Zang J, Wang Y, Zhang S, Wu P, Chen W, Shi L, Wu Y, Deng D, Cai K, Mai H, Xu A and Lu D. IGF2BP1 positively regulates CircOGDH accumulation in hypoxia induced stress granules. Acta Pharm Sin B 2025; 15: 6478-6494.
[37] Wei C, Peng D, Jing B, Wang B, Li Z, Yu R, Zhang S, Cai J, Zhang Z, Zhang J and Han L. A novel protein SPECC1-415aa encoded by N6-methyladenosine modified circSPECC1 regulates the sensitivity of glioblastoma to TMZ. Cell Mol Biol Lett 2024; 29: 127.
[38] Li X, Yang G, Ma L, Tang B and Tao T. N(6)-methyladenosine (m(6)A) writer METTL5 represses the ferroptosis and antitumor immunity of gastric cancer. Cell Death Discov 2024; 10: 402.

Supplementary Table 1. The RT-qPCR primers in this research

Gene	Primers sequences	
CircSLIT2	Forward	5'-TAGAACTCTATCGGGGGCGT-3'
	Reverse	5'-TGTTGCTACAGGTACAGGCG-3'
SNX10	Forward	5'-CACTTTTGCTTTCAGATAGCAGC-3'
	Reverse	5'-ACACACGCCTCAATGTCTTCT-3'
LGALS8	Forward	5'-ATCTATAACCCGGTAATCCCGTT-3'
	Reverse	5'-CATGCCCACGTATCACAATCAA-3'
DIAPH1	Forward	5'-CTTGCGGGATATGCCTCTG-3'
	Reverse	5'-AATGTTTGCACCCAACTGACA-3'
SH3GLB1	Forward	5'-CAGGAACAGCTTATGGTAATGCC-3'
	Reverse	5'-GGCTGACGTTTGAATCAGTTCTC-3'
SBNO1	Forward	5'-CCAGGGCAAGATTTACTGCTT-3'
	Reverse	5'-AAGTGGCACTGACTGCTGAAC-3'
ARID5B	Forward	5'-TCTTAAAGGCAGACCACGCAA-3'
	Reverse	5'-TGCCATCGGAATTGTTGTTGG-3'
MIA3	Forward	5'-GGCCCGGATTGTCGTTTTG-3'
	Reverse	5'-GCCATCCTCTTGCCAGTTTAT-3'
LIN7C	Forward	5'-GAAGTGAGAGCGAACGCTACT-3'
	Reverse	5'-TCCACCTGGAATTATTCGGGAT-3'
ABHD2	Forward	5'-CATGCTGGAGACTCCCGAAC-3'
	Reverse	5'-CAAACACCGGACGATCACGTA-3'
SLIT2	Forward	5'-GCGAAGCTATACAGGCTTGAT-3'
	Reverse	5'-TGCAGTCGAAAAGTCCTAAGTTT-3'
METTL3	Forward	5'-TTGTCTCCAACCTTCCGTAGT-3'
	Reverse	5'-CCAGATCAGAGAGGTGGTGTAG-3'
METTL14	Forward	5'-AGTGCCGACAGCATTGGTG-3'
	Reverse	5'-GGAGCAGAGGTATCATAGGAAGC-3'
WTAP	Forward	5'-CTTCCCAAGAAGGTTCGATTGA-3'
	Reverse	5'-TCAGACTCTCTTAGGCCAGTTAC-3'
ALKBH5	Forward	5'-CGGCGAAGGCTACACTTACG-3'
	Reverse	5'-CCACCAGCTTTTGGATCACCA-3'
FTO	Forward	5'-ACTTGGCTCCCTTATCTGACC-3'
	Reverse	5'-TGTGCAGTGTGAGAAAGGCTT-3'
β-actin	Forward	5'-CATGTACGTTGCTATCCAGGC-3'
	Reverse	5'-CTCCTTAATGTCACGCACGAT-3'

Supplementary Table 2. RNAi sequences applied in this study

Gene	siRNA sequences	
circSLIT2-KD1	sense strand	5’-UGCAAAACACUACAAGAAGGA-3’
	antisense strand	5’-CUUCUUGUAGUGUUUUGCACU-3’
circSLIT2-KD2	sense strand	5’-AUUGUGUUCUGUUCCAAACGU-3’
	antisense strand	5’-GUUUGGAACAGAACACAAUCA-3’
METTL14 -KD1	sense strand	5’-AAAAGUACUAGAAUCUUUGUA-3’
	antisense strand	5’-CAAAGAUUCUAGUACUUUUCU-3’
METTL14 -KD2	sense strand	5’-AGGAUAUUCUUCAAAUCUGUC-3’
	antisense strand	5’-CAGAUUUGAAGAAUAUCCUAA-3’
SH3GLB1-KD1	sense strand	5’-UCCAUAUUUUGGUACAUUCAG-3’
	antisense strand	5’-GAAUGUACCAAAAUAUGGACA-3’
SH3GLB1-KD2	sense strand	5’-UAUAUUGUCCCAAAAGUUCUG-3’
	antisense strand	5’-GAACUUUUGGGACAAUAUAUG-3’
IGF2BP1-KD1	sense strand	5’-UUUUUGUCUCGGUAUCUUGCU-3’
	antisense strand	5’-CAAGAUACCGAGACAAAAAUC-3’
IGF2BP1-KD2	sense strand	5’-ACAUUAAGGUCAAGAAAUGAA-3’
	antisense strand	5’-CAUUUCUUGACCUUAAUGUUU-3’
siRNA-NC	sense strand	5’-UUCUCCGAACGUGUCACGU-3’
	antisense strand	5’-ACGUGACACGUUCGGAGAA-3’

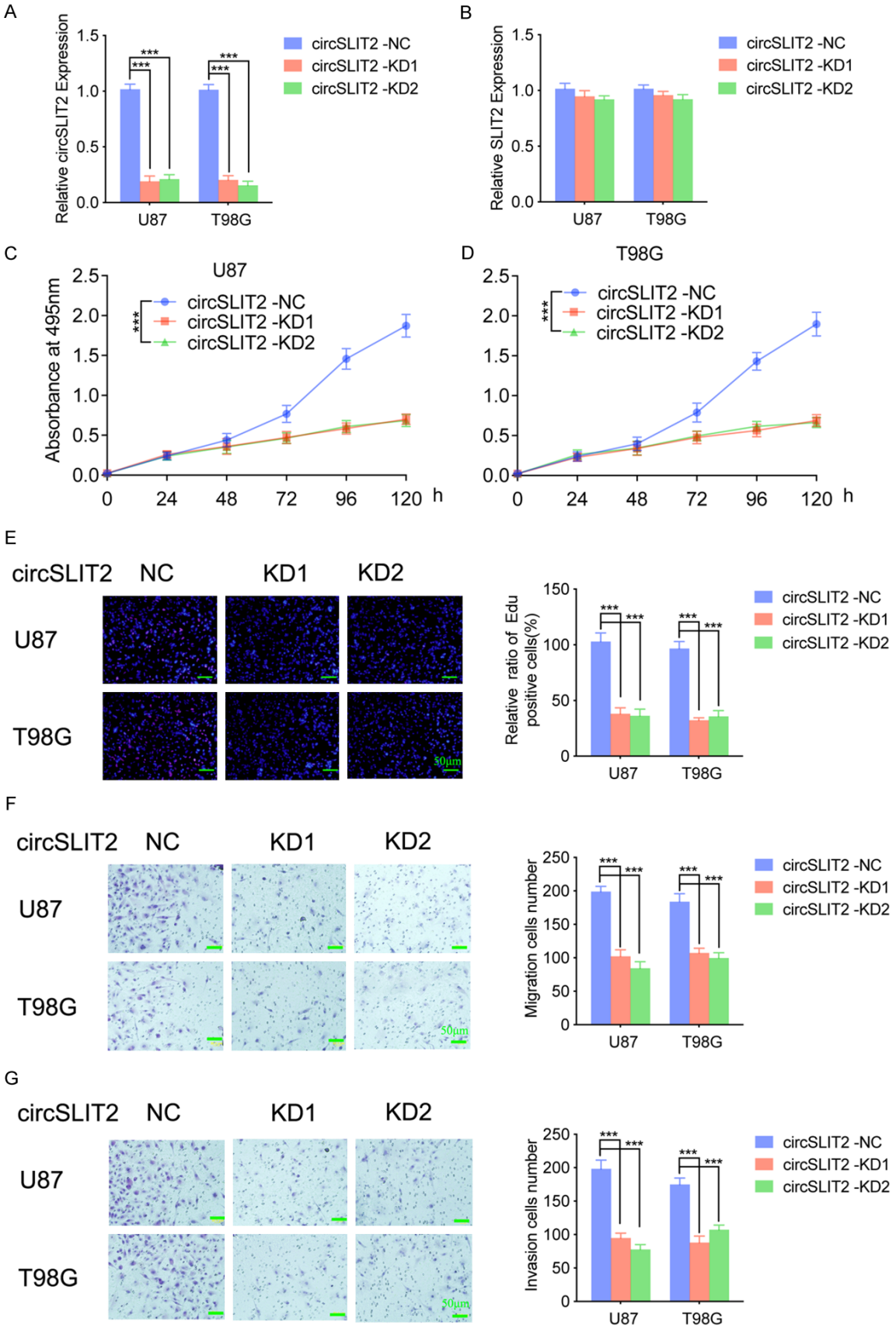
A
Relative circSLIT2 Expression
1.5
1.0
0.5
0.0
***
***
***
***
U87
T98G
circSLIT2 -NC
circSLIT2 -KD1
circSLIT2 -KD2
B
Relative SLIT2 Expression
1.5
1.0
0.5
0.0
U87
T98G
circSLIT2 -NC
circSLIT2 -KD1
circSLIT2 -KD2
C
U87
Absorbance at 495nm
2.5
2.0
1.5
1.0
0.5
0.0
***
circSLIT2 -NC
circSLIT2 -KD1
circSLIT2 -KD2
0
24
48
72
96
120
h
D
T98G
2.5
2.0
1.5
1.0
0.5
0.0
***
circSLIT2 -NC
circSLIT2 -KD1
circSLIT2 -KD2
0
24
48
72
96
120
h
E
circSLIT2
NC
KD1
KD2
U87
T98G
50μm
Relative ratio of Edu positive cells(%)
150
100
50
0
***
***
***
***
U87
T98G
circSLIT2 -NC
circSLIT2 -KD1
circSLIT2 -KD2
F
circSLIT2
NC
KD1
KD2
U87
T98G
50μm
Migration cells number
250
200
150
100
50
0
***
***
***
***
U87
T98G
circSLIT2 -NC
circSLIT2 -KD1
circSLIT2 -KD2
G
circSLIT2
NC
KD1
KD2
U87
T98G
50μm
Invasion cells number
250
200
150
100
50
0
***
***
***
***
U87
T98G
circSLIT2 -NC
circSLIT2 -KD1
circSLIT2 -KD2

Supplementary Figure 1. Knockdown of circSLIT2 inhibits the proliferative, migratory, and invasive capacities of glioma cells in vitro. (A, B) Validation of circSLIT2 knockdown efficiency and specificity in U87 and T98G cells. (A) qRT-PCR results showed that transfection with two independent circSLIT2-targeting siRNAs (circSLIT2-KD1 and circSLIT2-KD2) significantly downregulated circSLIT2 expression compared with the negative control (circSLIT2-NC). (B) The expression of linear SLIT2 mRNA remained unchanged in circSLIT2-knockdown cells, confirming the specificity of the knockdown. (C, D) MTS assay measuring absorbance levels after circSLIT2 knockdown in U87 (C) and T98G (D) cells. (E) EDU assay detecting changes in the EDU-positive rate after circSLIT2 knockdown in U87 and T98G cells (With magnification of 20×). Scale bar = 50 μm. (F, G) Transwell (F) and migration (G) assays measuring the number of invasive and migrating cells after circSLIT2 knockdown in U87 and T98G cells (With magnification of 20×). Scale bar = 50 μm. All data are shown as the mean ± SD (three independent experiments). *P < 0.05; **P < 0.01; ***P < 0.001.

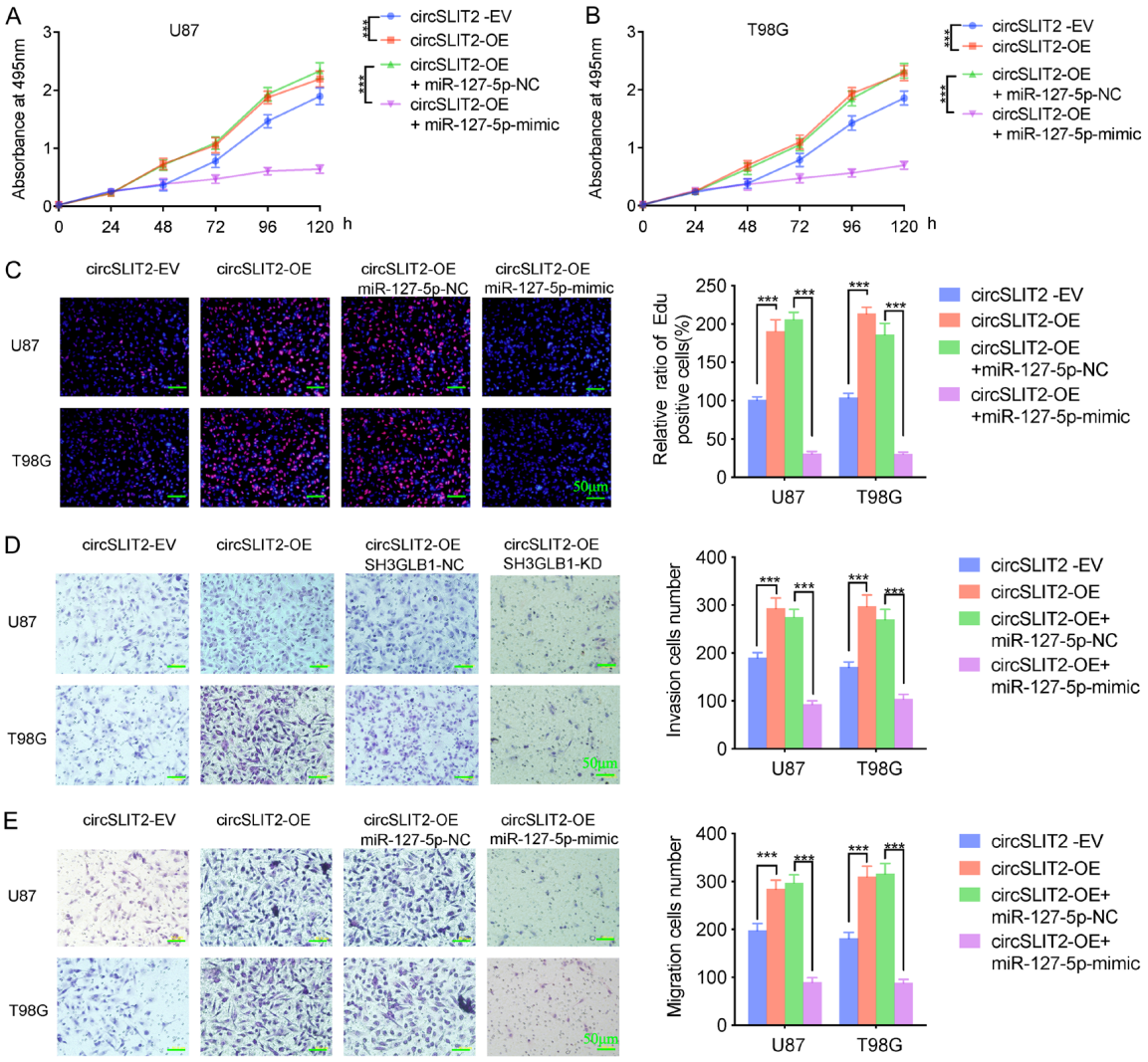

Supplementary Figure 2. CircSLIT2 promotes the malignant phenotype of glioblastoma cells via miR-127-5p. (A, B) MTS assay measuring changes in absorbance levels in U87 (A) and T98G (B) cells overexpressing circSLIT2 after treatment with miR-127-5p mimic. Scale bar = 50 μm. (C) EDU assay detecting changes in EDU-positive cell rates in U87 and T98G cells overexpressing circSLIT2 after treatment with miR-127-5p mimic (With magnification of 20×). Scale bar = 50 μm. (D, E) Transwell and migration assays showing changes in cell invasion (D) and migration (E) in U87 and T98G cells overexpressing circSLIT2 after treatment with miR-127-5p mimic (With magnification of 20×). Scale bar = 50 μm. All data are shown as the mean ± SD (three independent experiments). *P < 0.05; **P < 0.01; ***P < 0.001.

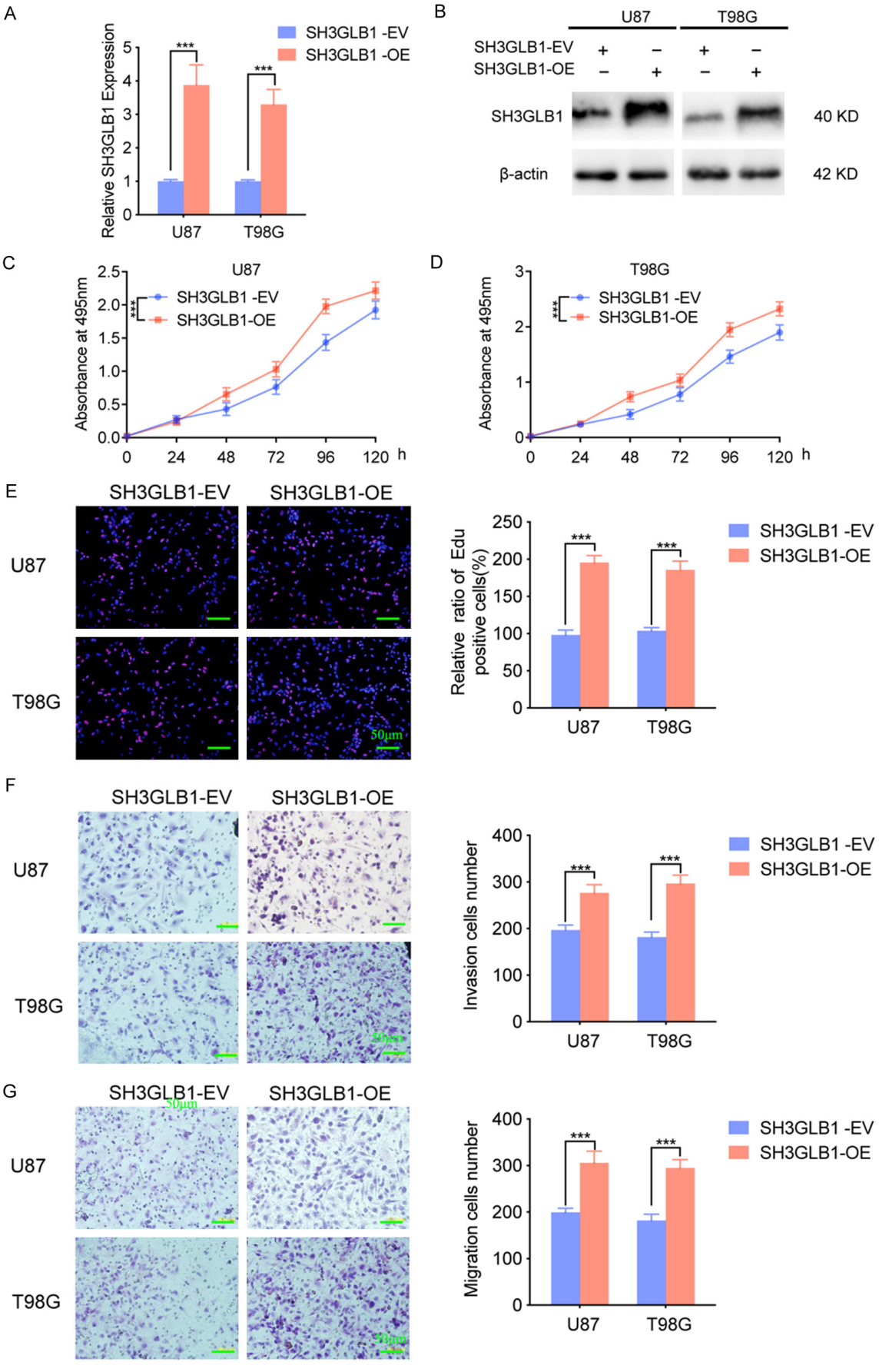
A
Relative SH3GLB1 Expression
SH3GLB1 -EV
SH3GLB1 -OE
***
U87
T98G
B
U87
T98G
SH3GLB1-EV
SH3GLB1-OE
SH3GLB1
40 KD
β-actin
42 KD
C
U87
Absorbance at 495nm
SH3GLB1 -EV
SH3GLB1-OE
h
D
T98G
E
SH3GLB1-EV
SH3GLB1-OE
U87
T98G
50μm
Relative ratio of Edu positive cells(%)
F
Invasion cells number
G
Migration cells number

Supplementary Figure 3. SH3GLB1 promotes the malignant phenotype of glioblastoma cells. (A, B) qPCR (A) and western blotting (B) analysis of SH3GLB1 overexpression efficiency in glioblastoma cell lines U87 and T98G. (C, D) MTS assay measuring absorbance levels after SH3GLB1 overexpression in glioblastoma cell lines U87 and T98G. (E) EDU assay detecting changes in the EDU-positive rate after SH3GLB1 overexpression in glioblastoma cell lines U87 and T98G (With magnification of 20×). Scale bar = 50 μm. (F, G) Transwell (F) and migration (G) assays measuring the number of invasive and migrating cells after SH3GLB1 overexpression in glioblastoma cell lines U87 and T98G (With magnification of 20×). Scale bar = 50 μm. All data are shown as the mean ± SD (three independent experiments). *P < 0.05; **P < 0.01; ***P < 0.001.